

3D Stress Intensity Factor evaluation by Dual BEM

A. Apicella #, R. Citarella*, A. Soprano *

Alenia un'Azienda Finmeccanica, Pomigliano d'Arco (NA), Italy

*Dipartimento di Progettazione e Gestione Industriale, Università degli Studi di Napoli Federico II
P.le Tecchio 80, 80125 Napoli, Italy

Abstract

This work, realized in the context of BRITE-EURAM (SMAAC) project, concerns a study on numerical evaluation of linear elastic crack 3D problems, using a Single-Domain Boundary Element Method and in particular the Dual Boundary Element Methodology. The method, implemented in a commercial code (BEASY), uses both the conventional Displacement Integral Equation and the less commonly used Traction Integral Equation and relies on the use of discontinuous elements to model the cracks. SIF's on a circular quadrant crack have been evaluated with reference to a two hole plate undergoing different loading conditions.

1. Introduction

The Boundary Element Method (BEM) is now well established in many engineering disciplines as an effective alternative to the Finite Element Method. The main attraction of BEM is largely attributed to the reduction in the dimensionality of the problem; for three-dimensional problems only the surface of the domain needs to be discretized. This means that compared to domain type analysis, a boundary element analysis results in a substantial reduction in data preparation and a much smaller system of algebraic equations to be solved numerically. However this advantage is sometimes overcome by the fact that the system of equations generated by BEM is fully populated and non symmetric. As the solution time for this type of system matrix is proportional to a cubic power of the total number of degrees of freedom, the required computational time can become large for complex structural models. Since the procedures developed for FEM generally assume a particular type of matrix, (i.e. symmetric, positive definite (SPD), sparse with small bandwidth), new solution strategies are required to solve the different type of matrix produced by BEM.

In the construction of large, complex models it is often more economical to split the model into smaller simpler sub-models. These sub-models or regions, which may also have different material properties, are modelled independently and then joined together along an interface. This strategy leads to an overall system matrix which has a blocked and unsymmetric character. This characteristic of multi-region formulation significantly extends the range of problems that can be solved, due to the large savings in storage and CPU required to solve the matrix compared with a fully populated matrix. However, the sparsity of such matrices is of a different type to that of FEM matrices. This has led to research being concentrated on the direct method for solving matrices, characterized by the factorization of the system matrix by Gauss elimination or by Choleski's method. Other methods have also been used in conjunction with direct methods to reduce the amount of space required for the system matrix.

2. Theoretical aspects of Dual Boundary Element Method

There follows a summary of the Single-Domain Boundary Element Method and in particular the Dual Boundary Element Methodology, detailed in references [1] for 2D and [2] for 3D applications, adopted for the numerical evaluation of linear elastic crack problems using boundary integral equations with discontinuous elements. The method uses both the conventional Displacement Integral Equation (the free term of which involves displacement at the source point)

and the less commonly used Traction Integral Equation (the free term of which involves traction at the source point). Actually, the Displacement Equation alone does not provide a viable method for single domain analysis of general crack problems, because of the coefficient matrix ill-conditioning (there is not a sufficient number of independent equations). This drawback can be circumvented by adopting two independent equations on the two crack edges.

2.1. Boundary Integral Equations

Define spatial coordinates x_i (subscript $i=1-3$), with source point x_i^* . Displacement $u_i(\mathbf{x})$ and traction $t_i(\mathbf{x})$ on the boundary S of a three-dimensional solid are related by the displacement BIE (1) and traction BIE (2) (three components $j=1-3$) for a source point on a smooth boundary S

$$\frac{1}{2} \delta_{ij} u_j(x^*) + \int_S \bar{T}_{ij}(x^*, x) u_j(x) dS(x) - \int_S U_{ij}(x^*, x) t_j(x) dS(x) = 0 \quad (1)$$

$$\frac{1}{2} t_j(x^*) - n_i(x^*) \int_S \bar{D}_{kij}(x^*, x) t_k(x) dS(x) + n_i(x^*) \int_S \bar{S}_{kij}(x^*, x) u_k(x) dS(x) = 0 \quad (2)$$

where the summation convention is assumed for repeated suffices. This is a limiting form of the BIE characterized by a source point interior to the boundary S and the kernel functions $T_{ij}(\mathbf{x}^*, \mathbf{x})$ and $D_{kij}(\mathbf{x}^*, \mathbf{x})$ are $O(r^{-2})$ singular while $S_{kij}(\mathbf{x}^*, \mathbf{x})$ is $O(r^{-3})$ singular. The two symbols \int_S^- , \int_S^+ stand

respectively for the Cauchy and Hadamard principal value integrals.

In the displacement and traction equation, apparently singular terms arise due to the presence of the source point on the boundary. Provided that certain continuity conditions hold for the surface variables (displacement and traction) at the source point, no singularities actually exist and the integral equations are well defined.

2.2. Discontinuous elements

Application of conventional Boundary Element Method with continuous element to the hypersingular traction equation fails due to the unsuitable representation of the surface displacement and traction at the nodal source points. The numerical solutions will not converge unless the assumed form of displacement and traction on the boundary element adjoining the source point comply with the following conditions: displacement and traction assumed on the boundary elements must be respectively C^1 and C^0 -continuous at the boundary source point. The necessary conditions for the existence of the principal value integrals obtained in the derivation of the dual boundary integral equations impose restrictions on the discretization. Actually, in the traction equation the continuity requirements of the Hadamard principal value integral are satisfied only by discontinuous elements, since all the nodes are internal points of the element where a continuous differential approximation is defined. Moreover, the requirement of the smoothness of geometry at a collocation point in the traction equation is implicitly satisfied by the discontinuous element.

2.3. Crack modelling

The general modelling strategy can be summarised as follows:

- the traction equation (2) is applied for collocation on one of the crack boundaries;
- the displacement equation (1) is applied for collocation on the opposite crack boundary and remaining boundaries;
- the crack boundaries are discretized with discontinuous boundary elements;
- continuous quadratic boundary elements are used along the remaining boundaries of the problem domain, except at the intersection between a crack and an edge, where discontinuous or semi-discontinuous elements are required, in order to avoid nodes at the intersection.

2.4. Stress intensity factors evaluation

Special discontinuous quadratic boundary elements [3] are used along the crack front, and values of Stress Intensity Factors (SIF's) are derived from the crack opening displacement on such elements, by using the BEASY code (developed at the Wessex Institute of Technology in Southampton (UK) and well suited for 3D SIF's evaluation [4,5]).

3 Solved problems

A large rectangular plate of overall size $-B < x_1 < +B$, $-H < x_2 < +H$, $-h/2 < x_3 < h/2$ contains two cracked holes. Values of tensile modulus $E=72000$ and Poisson's ratio $\nu = 0.3$ are assumed. The hole radius is $R=2.0$ mm and the hole pitch is $P=20.0$ mm. The plate dimensions $2B$ and $2H$ are chosen to simulate an infinite panel and the plate thickness is $h=1.6$ mm.

The structural configuration considered is based on one hole with a quadrant crack of radius $a_1=0.8$ mm and a nearby through-crack, emanating from an adjacent hole of length $a_2=8.0$ mm, with a panel size of $2B=2H=160$ mm (Fig.1).

The loading cases considered are:

- uniform remote tension $S=100$ N/mm² applied as tractions on the end surface $x_2=+H$, while the other end surface is suitably constrained. SIF's values for the quadrant cracks are normalized by $K_0 = S \sqrt{\pi \cdot a_1 / Q}$, where $Q=2.464$ as in [6]. SIF's values for the straight fronted cracks are normalized by $K_0 = S \sqrt{\pi \cdot a_2}$;
- uniform remote bending $\sigma_{22} = S (2 x_3 / h)$ is applied by means of tractions t_2 acting on the end surfaces $x_2=\pm H$. SIF's values for quadrant cracks are normalized as in the traction case;

The boundary element mesh used for the quadrant crack corresponds to 6 uniform divisions in the angular direction and 4 divisions in the radial direction, while for the through crack it corresponds to 6 uniform divisions in x_3 direction and 5 divisions in x_1 direction. The boundary mesh is illustrated in Figg. 2a-b.

In the case of uniform remote tension, 3-dimensional numerical solutions have been obtained using a fixed number of elements (about 2000), with a p-convergence study realized by gradually augmenting the element order in the zone surrounding the crack, from linear to reduced quadratic. Run times were varying between 2 hours (12396 dof) and 12 hours (17085 dof). Increasing the order of elements to "reduced" quadratics (8 nodes per element) around the cracks, produced a slight SIF's variation (less than 7%), except at the ends of the through crack front where the differences can be considerable. Negligible changes in the solution were produced by setting up the element subdivision option, applied to the most refined mesh adopted (less than 1%). Using an increased number of subdivision in the angular and radial direction for the quadrant crack had a negligible effect on the results, as for the through crack increasing the number of subdivision in x_3 direction. Care has been taken in removing only the degrees of freedom related to rigid body displacement, even if, completely clamping the plate on one side will not affect significantly the results. SIF's for the quadrant cracks are depicted in Fig.3, Table 1. Von Mises stress around the two holes are shown in Fig. 4.

For the bending case, the same mesh has been adopted but with a convergence study starting from 8-noded elements (26400 dof) up to 9-noded elements (32388) throughout the whole domain (the application of linear elements is practically useless). This time the element subdivision option, applied to the most refined mesh, has been useful to improve the accuracy, showing the need to continue the convergence study. Run times were varying from about 20 to 48 hours. In Figg. 5a-c Von Mises stresses are well evident on the overall plate and around the cracks whose opening in the deformed plate is also shown. Normalised SIF's for the quadrant crack are depicted in Fig. 6, Table 2, whilst for the straight-fronted crack they are not reported because affected by a considerable level of inaccuracy (up to 20%, [7,8]). In fact, it is evident from Fig. 5c that BEASY gives a non physical compenetration in the lower part of the straight crack, corresponding to compressive bending stresses (this is a code limitation that is not possible to circumvent), locally affecting the correct solution.

4. Conclusions

In conclusion some further remarks are due with regard to the opportunity, with a DBEM procedure, to model the zone surrounding the cracks with discontinuous elements, in such a way to simplify the meshing process and without loss of accuracy. Moreover it has been possible to reduce run times by zoning the whole plate in an adequate number of parts, paying attention to number consecutively the adjacent zones, in order to maximize benefits. Cubic elements have also been tested in the zone surrounding the cracks but without any improvement in accuracy. A satisfactory agreement of the results has been obtained compared with SMAAC partners [9,10] with a relatively small modelling effort. Further improvement in the BEASY code will be necessary in order to reduce computational times, even if we have to point out that the reported run-times are pessimistic because obtained with a compressed (roughly 20% longer run-times) and highly fragmented disk.

Bibliography

- [1] Portela A., Aliabadi M.H. & Rooke D.P. "Dual Boundary Incremental Analysis of Crack Propagation", *Int Journal Computers and Structures*, Vol.46, pp 237-247, 1993.
- [2] Mi, Y., Aliabadi, M.H., "Dual Boundary Element Method for Three Dimensional Fracture Mechanics Analysis", *Eng. Analysis with Boundary Elements*, Vol 10, 1992.
- [3] Mi Y., Aliabadi M.H., "Three-dimensional crack growth simulation using BEM", *Computers & Structures*, Vol 52, No 5, pp 871-878, (1994).
- [4] Beasy Crack Growth Guide Book, *Computational Mechanics BEASY*, Ashurst, Southampton, 1994.
- [5] A.C. Neves, R.A. Adey, J. M. W. Baynham and S. M. Niku, "Automatic 3D crack growth using BEASY", *Proceedings of BEM 19 Conference*, pp 819-827, *Computational Mechanics Publications*, Southampton, U.K. (1997).
- [6] P.W. Tan, J.C. Newman Jr and C.A. Bigelow "Three-dimensional finite element analysis of corner cracks at stress concentration", *Engineering Fracture Mechanics* 55, 502-505 (1996).
- [7] R.S. Alwar, K.N. Ramachandran Nambissan, "Influence of crack closure on the Stress Intensity Factor for plates subjected to bending – a 3D Finite Element Analysis", *Engineering Fracture Mechanics*, Vol. 17, No. 4, pp. 323-333, 1983 Pergamon Press Ltd.
- [8] M. V. V. Murthy, S. Viswanath, A.V. Krishna Murty, K. P. Rao, "A two dimensional model for crack closure effect in plates under bending", *Engineering Fracture Mechanics*, Vol. 29, No. 4, pp. 435-452, 1988 Pergamon Press plc.
- [9] J.P.M. Goncalves, P.T. de Castro, "Contribution to the Numerical Modeling of a Corner Crack at a Fastener Hole", Document No. SMAAC-WP-2.0-09-1.1/IDMEC.
- [10] A. Young, "Single-Domain Boundary Element Method for 3-D Elastostatic Crack Analysis", Document No. SMAAC-WP-2.0-07-1.0/DRA.

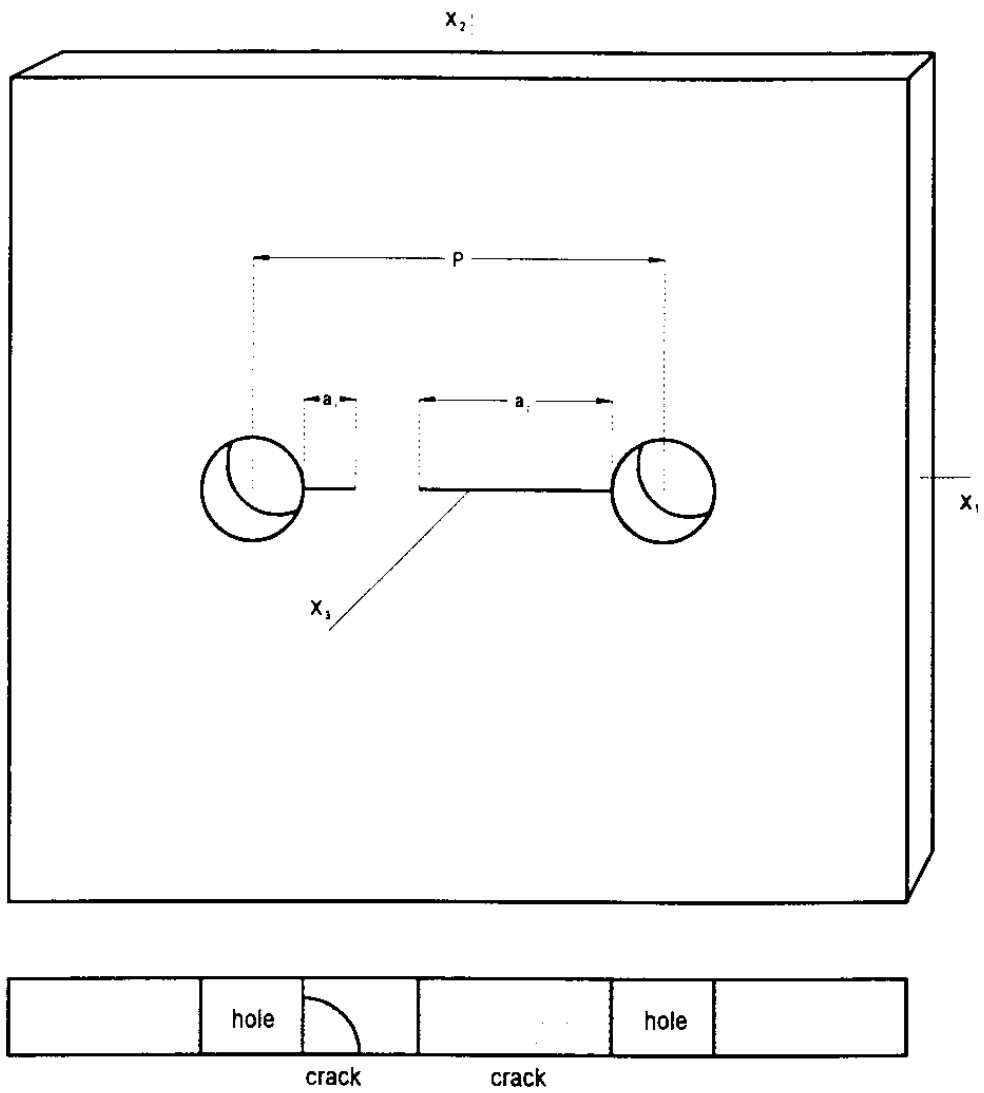


Figure1: Interacting cracks from two holes.

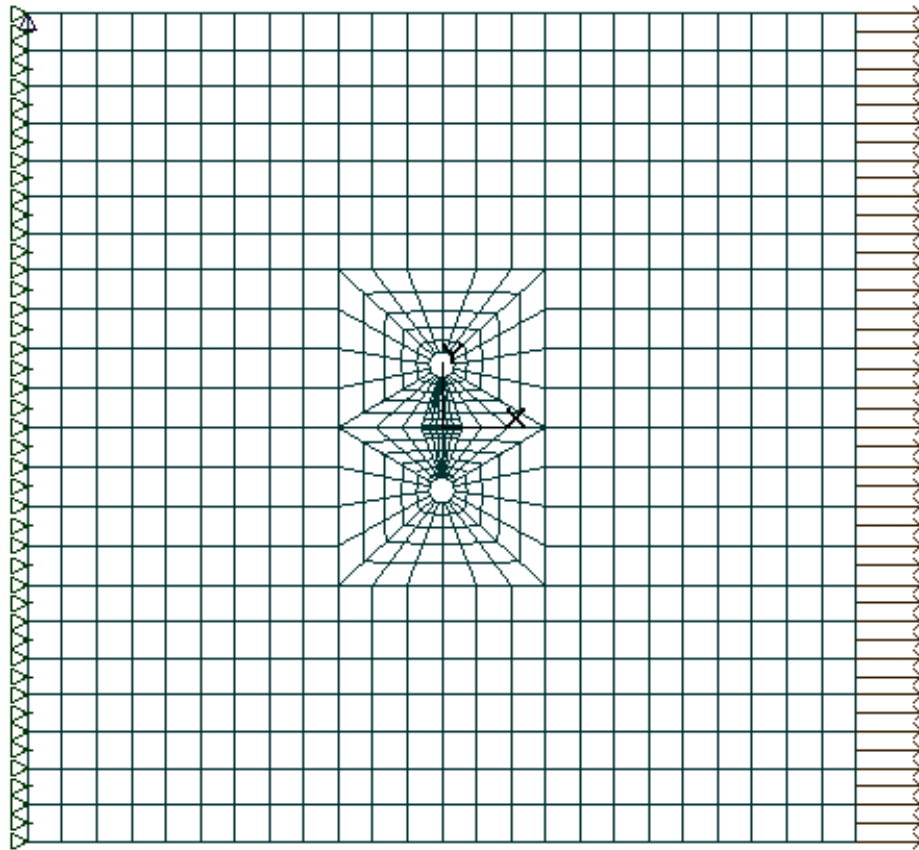


Figure 2a: overall boundary element mesh used for two hole plate.

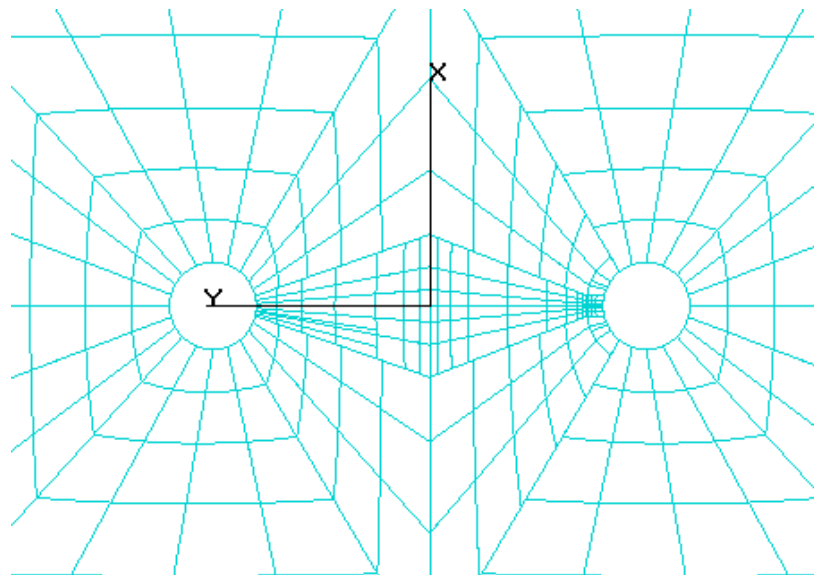


Figure 2b: close-up of boundary element mesh used for two hole plate.

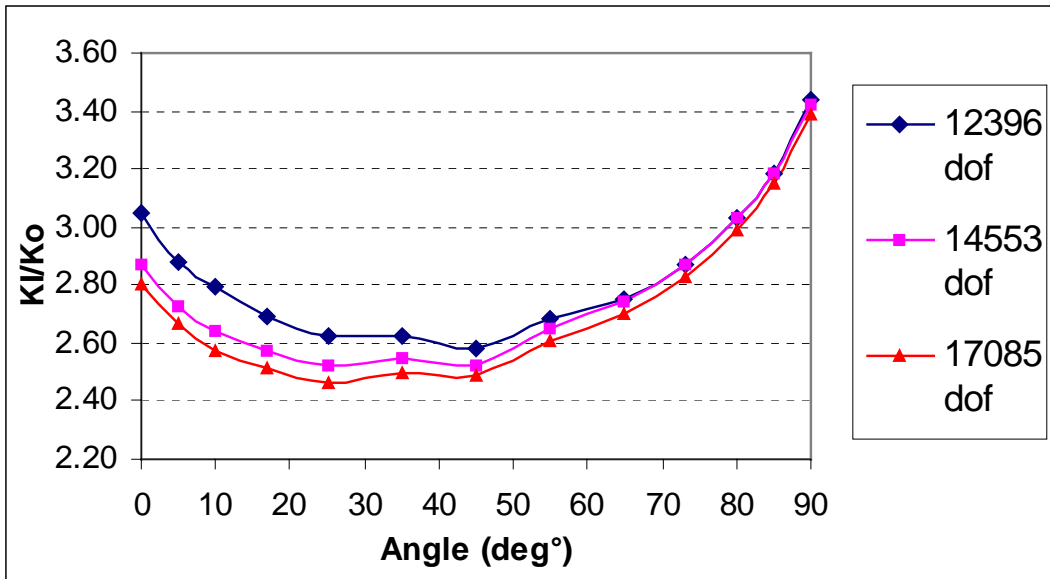


Figure 3: Normalized SIF's (K_I/K_0 , $K_0=101$) for quadrant crack ($a_1=0.8\text{mm}$) in traction case.

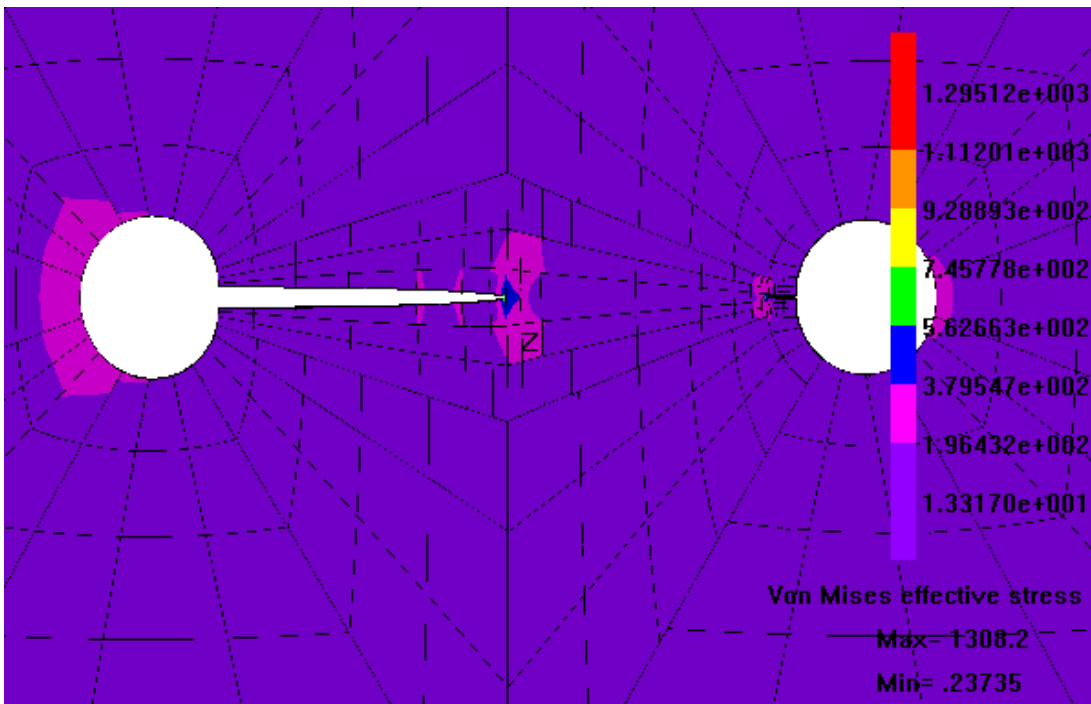


Figure 4: Stress state on a deformed plot, around the two holes ($R=2\text{mm}$) in traction case.

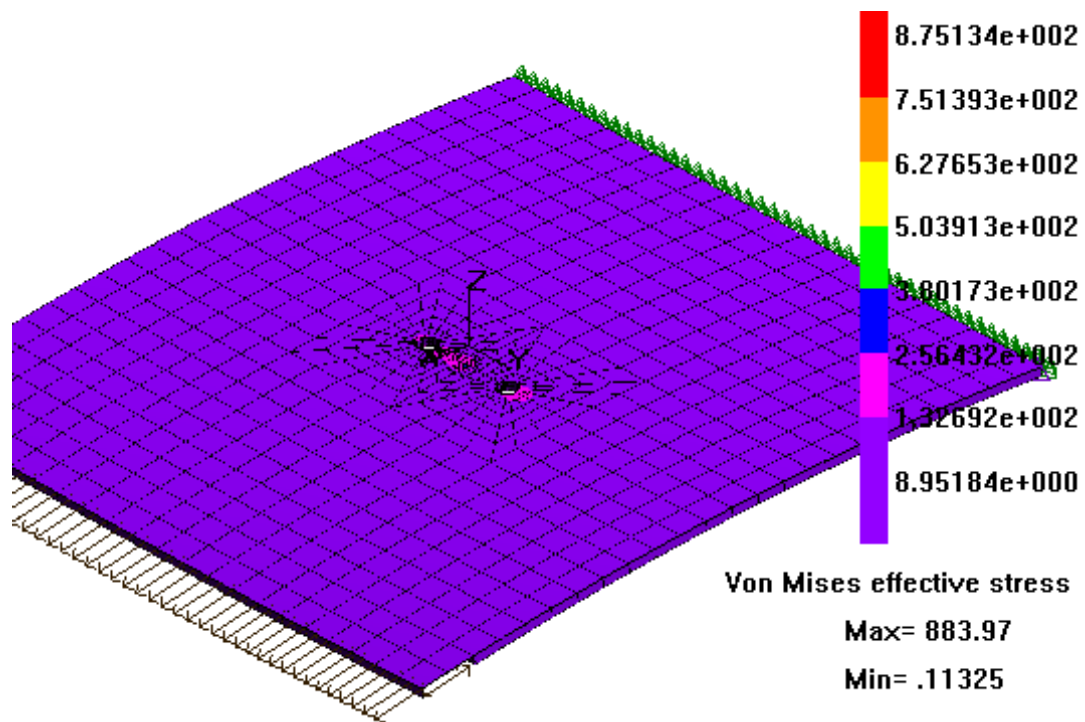


Figure 5a: overall stress state on plate deformed plot in bending case.

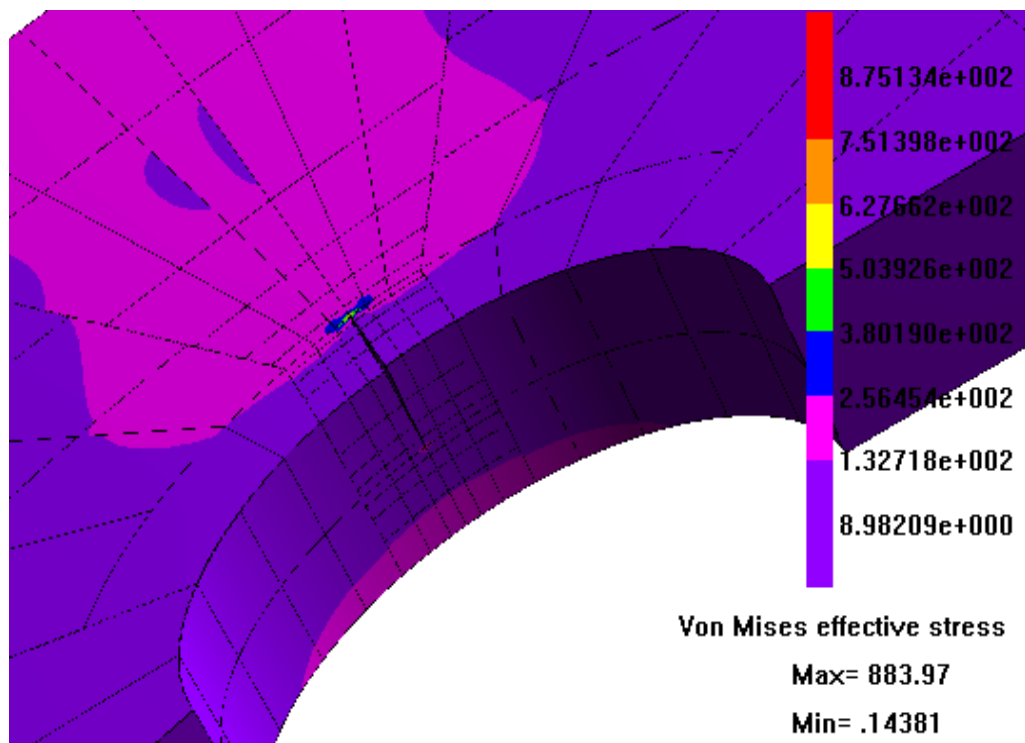


Figure 5b: close-up of the stress state around the quadrant crack ($a_1=0.8\text{mm}$) in bending case.

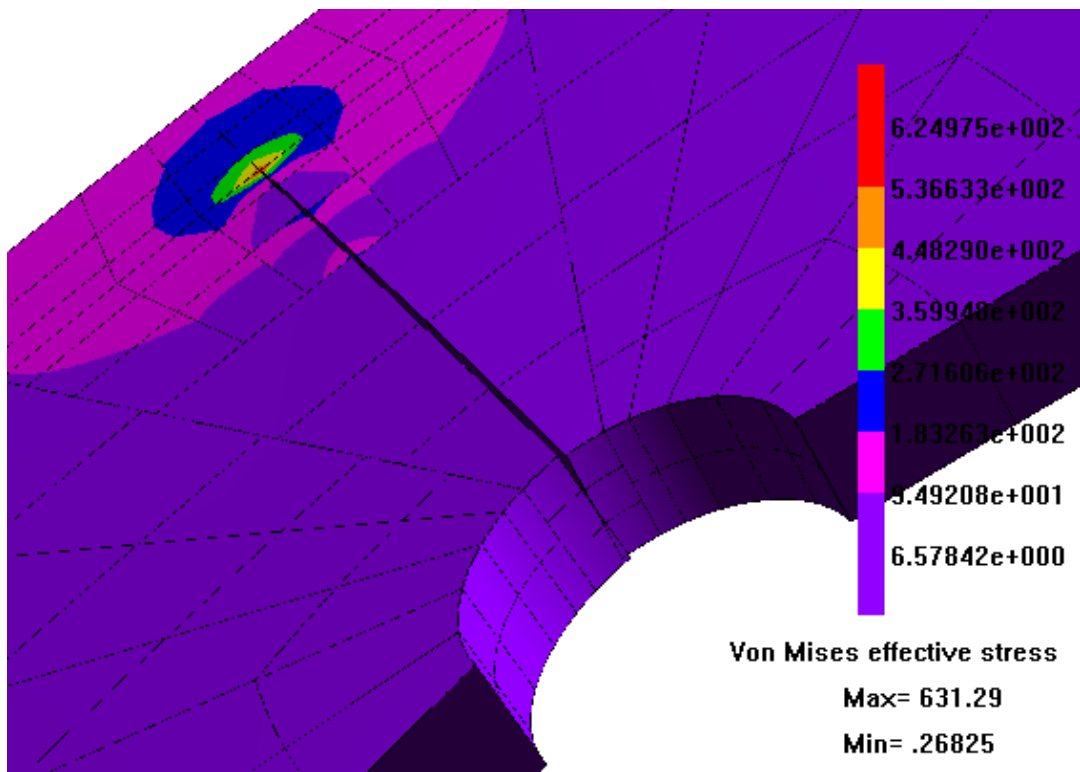


Figure 5c: close-up of the stress state around the through crack ($a_2=8\text{mm}$) in bending case.

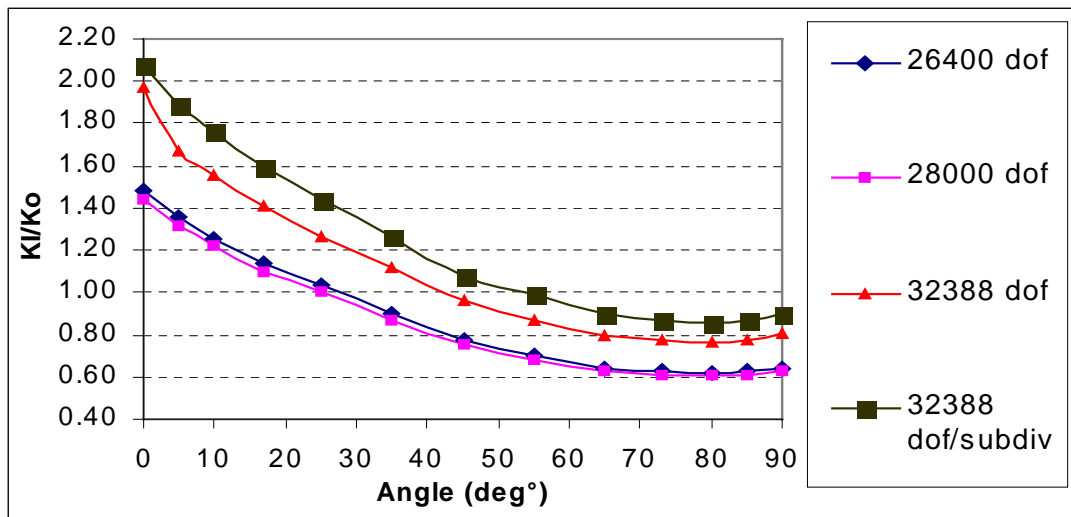


Figure 6: Normalized SIF's ($K_0=101$) for quadrant crack ($a_1=0.8\text{mm}$) in bending case.